Journal of Computational Applied Mechanics 2026, 57 (3): 425-442

DOI: 10.22059/jcamech.2026.412544.1799

RESEARCH PAPER

A Spectrally Accurate Shifted Lucas Collocation Framework for Fractional Lanchester Combat Dynamics with Time-Dependent Variable Coefficients

M.H. Salama [a], H.A. Zedan [a], W.M. Abd-Elhameed [b], Y.H. Youssri [b, c, d, *]

[a] *Department of Mathematics, Faculty of Science, Kafrelsheikh University, Kafrelsheikh 33516, Egypt*
[b] *Department of Mathematics, Faculty of Science, Cairo University, Giza 12613, Egypt*
[c] *Faculty of Engineering, Egypt University of Informatics, Knowledge City, New Administrative Capital 19519, Egypt*
[d] *Associate Fellow (AFHEA) of the Higher Education Academy (Advance HE), UK*

Abstract

This paper is confined to developing a rigorous computational framework using the shifted Lucas polynomials for the numerical treatment of the generalized fractional-order Lanchester combat model characterized by time-dependent variable coefficients. The method uses an exact operational matrix for the Caputo derivative to handle the singular kernel, thereby eliminating the need for numerical quadrature. A global polynomial projection at shifted Chebyshev–Gauss–Lobatto nodes eliminates predictor–corrector errors and preserves high-order accuracy under memory effects. A rigorous analysis employing a generalized Gronwall inequality establishes well-posedness and derives sharp stability bounds via Mittag–Leffler functions. Numerical investigations validate enhanced stability and efficiency, especially for memory effects and heavy-tail decay, and error estimates indicate super-geometric convergence.

Keywords: Fractional dynamical systems; Spectral collocation; Caputo derivative; Operational matrix; Coupled fractional ODEs; Mittag-Leffler stability; Numerical methods

MSC 2020: 34A08, 65M70, 91A80, 33C45, 26A33.

1. Introduction

The quantitative modeling of attrition dynamics remains a foundational pillar of military operations research, providing the analytical basis for force projection, resource allocation, and strategic wargaming. Since Frederick Lanchester's seminal work in 1916 [1], the deterministic "Square Law," formulated as a system of coupled Ordinary Differential Equations (ODEs), has served as the canonical paradigm for modern warfare analysis. While physically intuitive, the classical integer-order formulation relies on the "instantaneous exchange" hypothesis, assuming that attrition rates depend exclusively on the current state of forces [2]. This simplification neglects the hereditary nature of combat, in which a force's degradation is cumulative and shaped by the history of supply-chain latency, psychological fatigue, and tactical degradation.

To address these limitations, Fractional Calculus (FC) has emerged as a robust mathematical framework for modeling systems with non-local memory [3]. By replacing integer derivatives with fractional operators of order, the resulting Fractional Differential Equations (FDEs) naturally encode the weighted history of the engagement. Recent

* Corresponding author. Tel.: +20-100-187-5669.
E-mail address: youssri@cu.edu.eg

extensions of the Lanchester model have incorporated such memory effects to simulate heterogeneous attrition mechanisms and multi-stage conflict scenarios [4]. However, the introduction of realistic, time-dependent variable coefficients-representing phenomena such as diurnal effectiveness cycles or exponential resource exhaustion [5]-presents substantial analytical and computational challenges.

The singular behaviour of the fractional kernel near the origin is the main numerical issue with solving these systems. When solving integrals in long-term memory, conventional low-order approaches, such as the Adams-Bashforth-Moulton predictor-corrector schemes, experience significant order reduction and high computational cost [6]. In addition, stability degrades when variable coefficients are present, since traditional polynomial approximation methods often introduce "projection errors" when differentiating the basis functions.

Spectral methods, particularly those utilizing orthogonal polynomials, offer a powerful alternative due to their potential for exponential convergence [7, 8]. While Chebyshev and Legendre bases have dominated the literature, recent theoretical advances have highlighted the superior algebraic properties of Lucas polynomials for differential equations. The authors of [9] established novel connection formulae linking Lucas and Chebyshev bases, providing a robust theoretical foundation for their use in spectral solvers. This potential has been realized in very recent high-precision applications; the authors of [10] developed a rigorous Galerkin framework using modified shifted Lucas polynomials for the 2D Poisson equation, demonstrating exceptional spatial convergence. Similarly, Salama et al. [11] applied a Lucas-based collocation approach to the fractional Bratu equation, confirming the method's efficacy in handling nonlinear singularities.

Building upon this successful lineage [12-15], this paper proposes a Shifted Lucas Spectral Collocation Method (SLSCM) tailored for the variable-coefficient fractional Lanchester model. The principal contributions of this work are fourfold:

- **Exact Operational Matrix:** We derive a closed-form analytical expression for the Caputo fractional derivative of shifted Lucas polynomials involving Gauss hypergeometric functions. This formulation allows for the exact differentiation of the basis set, eliminating the truncation errors typically associated with numerical approximations of the fractional operator.

- **Rigorous Stability Analysis:** We extend the stability theory for combat models by analyzing the averaged non-autonomous system. Using Matignon's theorem [16] and Mittag-Leffler bounds [17], we prove the instability of the mutual annihilation equilibrium (Saddle Point), confirming the physical consistency of the fractional model.

- **Well-Posedness Theory:** Utilizing a generalized Gronwall inequality [18], we rigorously establish the existence, uniqueness, and continuous dependence of the solution on initial force strengths.

- **High-Order Efficiency:** We demonstrate that the proposed SLSCM achieves spectral accuracy for smooth solutions and maintains robust algebraic convergence for non-smooth fractional dynamics, significantly outperforming standard integrators (e.g., RK45, BDF) in terms of accuracy-per-computational-unit.

The remainder of the paper is organized as follows: Section 2 reviews the necessary definitions of fractional calculus and shifted Lucas polynomials. Section 3 details the construction of the exact operational matrix and the discretization of the variable-coefficient Lanchester system. Section 4 presents the well-posedness and continuous dependence analysis. Section 5 provides rigorous error analysis. Section 6 discusses stability analysis. Section 7 discusses numerical experiments, followed by conclusions in Section 8.

2. Mathematical Preliminaries

This section presents the essential definitions and results for the spectral collocation method. In addition, the Caputo derivative, shifted Lucas basis, and its operational matrix are accounted for.

2.1. The Caputo Fractional Derivative

For modeling physical systems with memory, the Caputo definition is advantageous as it accommodates standard initial conditions. In this work, we focus on the fractional order $\alpha \in (0,1)$, which corresponds to systems with sub-diffusive memory effects.

Definition 1. *For a function $y(t) \in AC[0,T]$, the Caputo fractional derivative of order $\alpha \in (0,1)$ is defined as [3]:*

$$D^{\alpha}y(t) = \frac{1}{\Gamma(1-\alpha)}\int_0^t \frac{y'(\tau)}{(t-\tau)^{\alpha}}\, d\tau, \tag{1}$$

where $\Gamma(\cdot)$ *denotes the Gamma function.*

A direct consequence of Definition 1 is that $D^{\alpha}C = 0$ for any constant C. Furthermore, the derivative of a monomial is given by the power rule:

$$D^{\alpha}t^{k} = \begin{cases} 0, & k = 0, \\ \dfrac{\Gamma(k+1)}{\Gamma(k+1-\alpha)}\, t^{k-\alpha}, & k \in \mathbb{N}. \end{cases} \tag{2}$$

2.2. Lucas and Shifted Lucas Polynomials

To construct a spectral method on the temporal domain $t \in [0,1]$, we employ the shifted Lucas polynomials. The classical Lucas polynomials meet the following recursive formula [19]:

$$L_m(x) = xL_{m-1}(x) + L_{m-2}(x), \qquad L_0(x) = 2,\ L_1(x) = x \quad m \geq 2, \tag{3}$$

Applying the affine transformation $x = 2t - 1$ yields the shifted Lucas polynomials that satisfy

$$L_m^*(t) = (2t-1)L_{m-1}^*(t) + L_{m-2}^*(t), \quad L_0^*(t) = 2,\ \ L_1^*(t) = 2t-1 \quad m \geq 2, \tag{4}$$

These polynomials can be expressed explicitly as power series, which is essential for deriving the fractional-derivative matrix.

Theorem 1. [20] *For any positive integer* m*, the shifted Lucas polynomial* $L_m^*(t)$ *can be expressed in the following form:*

$$L_m^*(t) = \sum_{k=0}^{m} c_{m,k}\ t^{k}, \tag{5}$$

With

$$c_{m,k} = (-1)^{m+k}\, 2^{k}\binom{m}{k}\, {}_2F_1\left(\begin{matrix}\frac{k-m}{2}, \frac{1+k-m}{2} \\ 1-m\end{matrix}\middle| -4\right). \tag{6}$$

Here, ${}_2F_1$ *denotes the Gauss hypergeometric function.*

3. Mathematical Modeling and Numerical Methodology

The spectral collocation procedure is followed in this section for the numerical treatment of the generalized fractional Lanchester combat model. A linear algebraic formulation is achieved by using the accurate operational matrix from Section 2 for the coupled fractional system.

3.1. The Generalized Fractional Lanchester System

We consider a generalized extension of the Lanchester modern warfare model, formulated in the fractional-order domain to incorporate memory effects inherent in complex attrition dynamics [4]. The system governs the temporal evolution of two opposing forces: the Air Defense units, denoted by $A(t)$, and the Swarm/Drone units, denoted by $S(t)$.

The combat dynamics are described by the following coupled system of Caputo fractional differential equations of order $\alpha \in (0,1]$:

$$\begin{aligned} D^{\alpha}A(t) &= -k_S(t)S(t) - \mu_A A(t), \quad t \in (0,T], \\ D^{\alpha}S(t) &= -k_A(t)A(t) - \mu_S S(t), \quad t \in (0,T], \end{aligned} \tag{7}$$

subject to the initial force strengths:

$$A(0) = A_0, \quad S(0) = S_0. \tag{8}$$

The parameters in this system carry specific operational interpretations [2]:

- Memory Index (α): The fractional order indicates the extent to which the dynamics of previous battles impact the attrition rate of the present. The fractional formulation accounts for cumulative historical factors, such as fatigue accumulation and delayed logistical effects, whereas the classical model with $\alpha = 1$ views losses solely as a function of the state.

- Operational Attrition (μ_A, μ_S): These constant coefficients represent non-combat losses due to mechanical failures, accidents, or desertion.

- Combat Effectiveness ($k_A(t), k_S(t)$): To simulate realistic dynamic scenarios, we consider time-varying effectiveness coefficients. Specifically, we examine periodic variations (modeling shift changes or environmental cycles) and exponential decay (modeling resource depletion or communication jamming) [5].

3.2. The Shifted Lucas Spectral Collocation Scheme (SLSCM)

We will employ a spectral collocation algorithm using the shifted Lucas polynomials as basis functions to numerically solve Eqs. (7)–(8). The main idea depends on utilizing the operational matrix to handle the fractional derivatives without projection errors.

A significant difficulty in treating FDEs is accurately representing the singular kernel $t^{-\alpha}$ near the origin. Standard methods often project the fractional derivative back onto the polynomial basis, introducing truncation errors that degrade global accuracy. To mitigate this, we adopt the exact analytical formula derived in [20].

Theorem 2. *Consider the shifted Lucas polynomial vector:*

$$\Phi(t) = [L_0^*(t), \dots, L_N^*(t)]^T, \tag{9}$$

and let $\alpha \in (0,1)$. *The following expression holds for the Caputo fractional derivative of* $\Phi(t)$*:*

$$D^{\alpha}\Phi(t) = t^{-\alpha}\left(\boldsymbol{U}^{(\alpha)}\Phi(t) - \boldsymbol{\rho}^{(\alpha)}\right), \tag{10}$$

where $\boldsymbol{U}^{(\alpha)}$ *is a square operational matrix of order* $(N+1)$ *and* $\boldsymbol{\rho}^{(\alpha)}$ *is a correction vector accounting for the initial values.*

The entries $\mathcal{U}_{n,j}^{(\alpha)}$ *of the matrix* $\boldsymbol{U}^{(\alpha)}$ *are given by:*

$$\mathcal{U}_{n,j}^{(\alpha)} = \sum_{s=n}^{j} \frac{s!\, c_{j,s}\, \lambda_{s,n}}{\Gamma(s-\alpha+1)}, \quad 0 \le n \le j \le N, \tag{11}$$

and $\mathcal{U}_{n,j}^{(\alpha)} = 0$ *for* $n > j$. *The correction vector entries are:*

$$\rho_j^{(\alpha)} = \frac{c_{j,0}}{\Gamma(1-\alpha)}. \tag{12}$$

Here, $c_{j,s}$ *are the expansion coefficients from Eq.* (5)*, and*

$$\lambda_{s,k} = \begin{cases} \dfrac{(-1)^{\frac{k-s}{2}}\, k!\, c_s}{2^k \left(\frac{k-s}{2}\right)! \left(\frac{k+s}{2}\right)!}\ {}_2F_1\left(\begin{matrix}\frac{1}{2}(-k-s), \frac{1}{2}(-k+s) \\ \frac{1}{2}\end{matrix}\,\middle|\, -\frac{1}{4}\right), & (s+k)\ \text{even}, \\ \dfrac{(-1)^{\frac{1}{2}(k-s-1)}\, k!\, c_s}{2^k \left(\frac{1}{2}(k-s-1)\right)! \left(\frac{1}{2}(k+s-1)\right)!}\ {}_2F_1\left(\begin{matrix}\frac{1}{2}(1-k-s), \frac{1}{2}(1-k+s) \\ \frac{3}{2}\end{matrix}\,\middle|\, -\frac{1}{4}\right), & (s+k)\ \text{odd}. \end{cases} \tag{13}$$

are the linearization coefficients representing the inverse expansion of power functions t^s *in terms of shifted Lucas polynomials* $L_n^*(t)$ *where*

$$c_s = \begin{cases} \frac{1}{2}, & s = 0 \\ 1, & s \geq 1 \end{cases} \tag{14}$$

In our numerical implementation, the operational matrix $\boldsymbol{D}^{(\alpha)}$ at the collocation nodes t_i is constructed point-wise as:

$$[\boldsymbol{D}^{(\alpha)}]_{ij} = [D^{\alpha} L_j^*(t)]_{t=t_i}, \quad i,j = 0, \dots, N. \tag{15}$$

3.2.1. Spectral Discretization

We approximate the state variables $A(t)$ and $S(t)$ using a truncated series of shifted Lucas polynomials $L_n^*(t)$ up to degree N:

$$A_N(t) = \sum_{j=0}^{N} a_j \, L_j^*(t), \quad S_N(t) = \sum_{j=0}^{N} s_j \, L_j^*(t), \tag{16}$$

where $\boldsymbol{a} = [a_0, \dots, a_N]^T$ and $\boldsymbol{s} = [s_0, \dots, s_N]^T$ are the unknown spectral coefficient vectors.

We will use the following shifted Chebyshev-Gauss-Lobatto collocation nodes mapped to $[0,1]$ to reduce Runge phenomenon interpolation errors [21].

$$t_i = \frac{1}{2}\left(1 - \cos\left(\frac{i\pi}{N}\right)\right), \quad i = 0,1, \dots, N. \tag{17}$$

that $t_0 = 0$ corresponds to the initial time, and $t_N = 1$ corresponds to the final time.

3.2.2. Algebraic System Assembly

Substituting the spectral approximations (16) into the governing equations and enforcing the residuals to vanish at the collocation points yields a discrete system. A critical feature of our approach is the handling of the singular kernel $t^{-\alpha}$ in the fractional derivative.

By utilizing the exact differentiation formula, Theorem 2, we construct the discrete differentiation matrix $\boldsymbol{D}^{(\alpha)}$ point-wise. Since the term $t^{-\alpha}$ is singular at $t_0 = 0$, we strictly partition the collocation conditions as follows:

I. Initial Condition Row ($i = 0$): The differential equations are replaced by the explicit initial conditions:

$$\sum_{j=0}^{N} a_j \, L_j^*(0) = A_0, \quad \sum_{j=0}^{N} s_j \, L_j^*(0) = S_0. \tag{18}$$

II. Dynamic Rows ($1 \leq i \leq N$): For all strictly positive time nodes ($t_i > 0$), the differential equations are enforced using the exact operational matrix entries:

$$\sum_{j=0}^{N} a_j \, [\boldsymbol{D}^{(\alpha)}]_{ij} + k_S(t_i) \sum_{j=0}^{N} s_j \, L_j^*(t_i) + \mu_A \sum_{j=0}^{N} a_j \, L_j^*(t_i) = 0, \tag{19}$$

and similarly for the equation governing $S(t)$.

This formulation leads to a global block-matrix system $\boldsymbol{\mathcal{M}}\boldsymbol{X} = \boldsymbol{F}$ for the composite unknown vector $\boldsymbol{X} = [\boldsymbol{a}^T, \boldsymbol{s}^T]^T$:

$$\begin{bmatrix} \boldsymbol{\mathcal{M}}_{AA} & \boldsymbol{\mathcal{M}}_{AS} \\ \boldsymbol{\mathcal{M}}_{SA} & \boldsymbol{\mathcal{M}}_{SS} \end{bmatrix} \begin{bmatrix} \boldsymbol{a} \\ \boldsymbol{s} \end{bmatrix} = \begin{bmatrix} \boldsymbol{F}_A \\ \boldsymbol{F}_S \end{bmatrix}. \tag{20}$$

The sub-matrices are constructed explicitly to account for the row replacement at $i = 0$:

- For $\boldsymbol{\mathcal{M}}_{AA}, \boldsymbol{\mathcal{M}}_{SS}$ blocks:

The first row ($i = 0$) contains the basis values at the initial time $[\boldsymbol{\mathcal{M}}_{AA}]_{0,j} = L_j^*(0)$. For dynamic rows ($i \geq 1$), the entries combine the fractional derivative and linear decay:

$$[\boldsymbol{\mathcal{M}}_{AA}]_{i,j} = [\boldsymbol{D}^{(\alpha)}]_{i,j} + \mu_A L_j^*(t_i). \tag{21}$$

- For $\boldsymbol{\mathcal{M}}_{AS}, \boldsymbol{\mathcal{M}}_{SA}$ blocks:

The first row ($i = 0$) is zero, as the initial conditions are uncoupled. For dynamic rows ($i \geq 1$), the entries represent the variable-coefficient coupling:

$$[\boldsymbol{\mathcal{M}}_{AS}]_{i,j} = k_S(t_i) L_j^*(t_i). \tag{22}$$

The right-hand side vectors are defined as $\boldsymbol{F}_A = [A_0, 0, \ldots, 0]^T$ and $\boldsymbol{F}_S = [S_0, 0, \ldots, 0]^T$.

4. Well-Posedness of the Fractional Lanchester System

Prior to the implementation of the spectral discretization, it is fundamental to establish the mathematical well-posedness of the governing continuous problem. In this section, we rigorously prove that the solution to the fractional Lanchester system exhibits continuous dependence on the initial data. This analysis is crucial not only for ensuring the existence and uniqueness of the solution but also for validating the physical consistency of the model against small perturbations in the initial force strengths.

Let $\boldsymbol{\mathcal{B}} = C([0,T]; \mathbb{R}^2)$ be the Banach space of continuous vector-valued functions equipped with the uniform norm. Consider two distinct solutions to the fractional system $\boldsymbol{u}(t)$ and $\tilde{\boldsymbol{u}}(t)$ where: $\boldsymbol{u}(t)$ is the exact solution satisfying $D^\alpha \boldsymbol{u}(t) = -\boldsymbol{M}(t)\boldsymbol{u}(t)$ subject to the initial condition $\boldsymbol{u}(0) = \boldsymbol{u}_0$, and $\tilde{\boldsymbol{u}}(t)$ is a perturbed solution satisfying the same dynamics but subject to $\tilde{\boldsymbol{u}}(0) = \boldsymbol{u}_0 + \boldsymbol{\delta}$, where $\boldsymbol{\delta} \in \mathbb{R}^2$ represents a small initial perturbation vector.

Theorem 3. *Assume that the combat effectiveness functions $k_A(t)$ and $k_S(t)$ are continuous and bounded on the interval $[0,T]$. Let $L = \sup_{t\in[0,T]} \| \boldsymbol{M}(t) \|_2 < \infty$. Then, for any initial perturbation $\boldsymbol{\delta}$, the error norm satisfies the following uniform bound for all $t \in [0,T]$:*

$$\| \boldsymbol{e}(t) \|_2 \leq \| \boldsymbol{\delta} \|_2 \, E_\alpha(Lt^\alpha), \tag{23}$$

where $E_\alpha(z) = \sum_{n=0}^{\infty} \frac{z^n}{\Gamma(n\alpha+1)}$ denotes the one-parameter Mittag-Leffler function.

Proof. Let $\boldsymbol{e}(t) = \tilde{\boldsymbol{u}}(t) - \boldsymbol{u}(t)$ denote the error vector. By linearity of the Caputo fractional derivative, the error dynamics are governed by the homogeneous system:

$$D^\alpha \boldsymbol{e}(t) = -\boldsymbol{M}(t)\boldsymbol{e}(t), \quad \boldsymbol{e}(0) = \boldsymbol{\delta}, \tag{24}$$

where the time-varying coefficient matrix is given by $\boldsymbol{M}(t) = \begin{bmatrix} \mu_A & k_S(t) \\ k_A(t) & \mu_S \end{bmatrix}$.

The proof relies on the construction of a convergent Picard sequence to establish the Generalized Gronwall Inequality [18].

We first convert the initial value problem (24) into an equivalent Volterra integral equation of the second kind. Applying the Riemann-Liouville fractional integral operator I^α to both sides and utilizing the fundamental theorem of fractional calculus ($I^\alpha D^\alpha \boldsymbol{e}(t) = \boldsymbol{e}(t) - \boldsymbol{e}(0)$), we obtain:

$$\boldsymbol{e}(t) = \boldsymbol{\delta} - \frac{1}{\Gamma(\alpha)} \int_0^t (t-\tau)^{\alpha-1} \boldsymbol{M}(\tau)\boldsymbol{e}(\tau) d\tau. \tag{25}$$

Taking the Euclidean norm of both sides, applying the triangle inequality, and using the consistency property of matrix norms ($\| \boldsymbol{Ax} \| \leq \| \boldsymbol{A} \| \| \boldsymbol{x} \|$), we arrive at:

$$\| \boldsymbol{e}(t) \|_2 \leq \| \boldsymbol{\delta} \|_2 + \frac{1}{\Gamma(\alpha)} \int_0^t (t-\tau)^{\alpha-1} \| \boldsymbol{M}(\tau) \|_2 \| \boldsymbol{e}(\tau) \|_2 \, d\tau. \tag{26}$$

Since the coefficient matrix is bounded by $\| \boldsymbol{M}(\tau) \|_2 \leq L$ uniformly on $[0,T]$, we establish the fundamental inequality:

$$\| \boldsymbol{e}(t) \|_2 \leq \| \boldsymbol{\delta} \|_2 + \frac{L}{\Gamma(\alpha)} \int_0^t (t-\tau)^{\alpha-1} \| \boldsymbol{e}(\tau) \|_2 \, d\tau. \tag{27}$$

Let $\psi(t) = \| \boldsymbol{e}(t) \|_2$. We solve the integral inequality $\psi(t) \leq \| \boldsymbol{\delta} \|_2 + I^{\alpha}(L\psi(t))$ using the method of successive approximations. Define the sequence of functions $\{\psi_n(t)\}_{n=0}^{\infty}$ iteratively as:

$$\begin{aligned} \psi_0(t) &= \| \boldsymbol{\delta} \|_2, \\ \psi_{n+1}(t) &= \| \boldsymbol{\delta} \|_2 + \frac{L}{\Gamma(\alpha)} \int_0^t (t-\tau)^{\alpha-1} \psi_n(\tau) d\tau. \end{aligned} \tag{28}$$

For the first iteration ($n = 0$):

$$\psi_1(t) = \| \boldsymbol{\delta} \|_2 + \frac{L \| \boldsymbol{\delta} \|_2}{\Gamma(\alpha)} \int_0^t (t-\tau)^{\alpha-1} d\tau = \| \boldsymbol{\delta} \|_2 \left(1 + \frac{Lt^{\alpha}}{\Gamma(\alpha+1)}\right). \tag{29}$$

For the second iteration ($n = 1$), substituting $\psi_1(t)$ into the integral:

$$\psi_2(t) = \| \boldsymbol{\delta} \|_2 + \frac{L}{\Gamma(\alpha)} \int_0^t (t-\tau)^{\alpha-1} \left[\| \boldsymbol{\delta} \|_2 + \frac{L \| \boldsymbol{\delta} \|_2 \, \tau^{\alpha}}{\Gamma(\alpha+1)} \right] d\tau. \tag{30}$$

Evaluating the convolution of power functions using the identity $\int_0^t (t-\tau)^{\alpha-1} \tau^{\beta} d\tau = \frac{\Gamma(\alpha)\Gamma(\beta+1)}{\Gamma(\alpha+\beta+1)} t^{\alpha+\beta}$, we obtain:

$$\psi_2(t) = \| \boldsymbol{\delta} \|_2 \left(1 + \frac{Lt^{\alpha}}{\Gamma(\alpha+1)} + \frac{(Lt^{\alpha})^2}{\Gamma(2\alpha+1)}\right). \tag{31}$$

Proceeding by mathematical induction, the n-th term of the sequence is given by the partial sum:

$$\psi_n(t) = \| \boldsymbol{\delta} \|_2 \sum_{k=0}^{n} \frac{(Lt^{\alpha})^k}{\Gamma(k\alpha+1)}. \tag{32}$$

Let $\mathcal{T}$ denote the Volterra integral operator on the right-hand side of (2ˇ), so that $\psi \leq \psi_0 + \mathcal{T}[\psi]$. Substituting this bound into its own right-hand side n times and using the monotonicity of $\mathcal{T}$ on non-negative functions gives $\psi(t) \leq \psi_n(t) + \mathcal{T}^{n+1}[\psi](t)$ for every $n \geq 0$. Since ψ is bounded on $[0,T]$ and the iterated kernel satisfies $\mathcal{T}^{n+1}[P](t) = P(Lt^{\alpha})^{n+1}/\Gamma\big((n+1)\alpha+1\big) \to 0$ as $n \to \infty$, the remainder vanishes and $\psi(t) \leq \lim_{n\to\infty} \psi_n(t)$. The series converges uniformly on any compact interval to the Mittag-Leffler function [17]:

$$\lim_{n\to\infty} \psi_n(t) = \| \boldsymbol{\delta} \|_2 \, E_{\alpha}(Lt^{\alpha}). \tag{33}$$

Consequently, $\| \boldsymbol{e}(t) \|_2 \leq \| \boldsymbol{\delta} \|_2 \, E_{\alpha}(Lt^{\alpha})$. Since $E_{\alpha}(z)$ is an entire function, it remains bounded for any finite t, which proves that the error depends continuously on the initial perturbation. Thus, the generalized fractional Lanchester model is well-posed. □

5. Convergence and Error Analysis

This section provides approximation-theoretic upper estimates for the truncation error of the shifted Lucas expansion. For Chebyshev–Gauss–Lobatto collocation, these bounds transfer to the discrete scheme up to the Lebesgue constant $\Lambda_n = O(\log N)$ [22]. Our study relies on two fundamental results that were developed in [20]

concerning the growth of shifted Lucas polynomials and the decay rate of spectral coefficients for analytic functions.

Lemma 1. *Let* $t \in [0,1]$. *The shifted Lucas polynomials satisfy the following inequality:*

$$|L_n^*(t)| \leq 2\phi^n, \qquad \forall n \geq 0, \tag{34}$$

where $\phi = \frac{1+\sqrt{5}}{2} \approx 1.618$ *represents the golden ratio.*

Theorem 4. *Let* $g(t)$ *be a function defined on* $[0,1]$ *such that its* n*-th derivative satisfies* $|g^{(n)}(0)| \leq \mu^n$ *for* $n > 0$, *where* $\mu > 0$ *is a constant. If* $g(t)$ *is expanded in terms of shifted Lucas polynomials as* $g(t) = \sum_{n=0}^{\infty} a_n L_n^*(t)$, *then the coefficients satisfy the asymptotic bound:*

$$|a_n| \lesssim \frac{\mu^n}{n!}. \tag{35}$$

We now establish the global truncation error bound for the proposed method. Let $A(t)$ be the exact solution of the Lanchester system, and let $A_N(t)$ be the approximate solution truncated at degree N.

Theorem 5 (Truncation Error Bound). *Assume that the exact solution* $A(t)$ *satisfies the analyticity condition* $|A^{(n)}(0)| \leq \mu^n$ *for some constant* $\mu > 0$. *Then, the truncation error* $E_N(t) = A(t) - A_N(t)$ *satisfies the following uniform error bound:*

$$\| A(t) - A_N(t) \|_{\infty} \leq \frac{2e^{\mu\phi}}{(N+1)!}(\mu\phi)^{N+1}, \tag{36}$$

where ϕ *is the golden ratio.*

Proof. The truncation error $E_N(t)$ is defined as the tail of the infinite series expansion:

$$E_N(t) = \sum_{n=N+1}^{\infty} a_n L_n^*(t). \tag{37}$$

Applying the triangle inequality and taking the absolute value:

$$|E_N(t)| \leq \sum_{n=N+1}^{\infty} |a_n||L_n^*(t)|. \tag{38}$$

We substitute the bounds provided by Lemma 1 and Theorem 4 into Eq. (38), we obtain:

$$|E_N(t)| \leq \sum_{n=N+1}^{\infty} \left(\frac{\mu^n}{n!}\right)(2\phi^n) = 2\sum_{n=N+1}^{\infty} \frac{(\mu\phi)^n}{n!}. \tag{39}$$

Let $X = \mu\phi$. The series becomes the tail of the Taylor expansion for the exponential function e^X:

$$|E_N(t)| \leq 2\sum_{n=N+1}^{\infty} \frac{X^n}{n!}. \tag{40}$$

This summation represents the remainder term $R_N(X)$ of the Maclaurin series for e^X. According to Taylor's theorem with the Lagrange form of the remainder, there exists some $\xi \in (0, X)$ such that:

$$R_N(X) = \sum_{n=N+1}^{\infty} \frac{X^n}{n!} = \frac{e^{\xi}}{(N+1)!}X^{N+1}. \tag{41}$$

Since the exponential function is strictly increasing and $\xi < X$, we have the upper bound $e^{\xi} < e^X$. Therefore:

$$\sum_{n=N+1}^{\infty} \frac{X^n}{n!} \leq \frac{e^X}{(N+1)!} X^{N+1}. \tag{42}$$

Substituting $X = \mu\phi$ back into the inequality, we arrive at the final error bound:

$$|E_N(t)| \leq 2\left(\frac{e^{\mu\phi}}{(N+1)!}(\mu\phi)^{N+1}\right). \tag{43}$$

Taking the supremum over $t \in [0,1]$, we obtain the uniform norm estimate:

$$\| E_N \|_\infty \leq \frac{2e^{\mu\phi}(\mu\phi)^{N+1}}{(N+1)!}. \tag{44}$$

This result demonstrates that the error decays factorially due to $(N+1)!$ in the denominator, which is significantly faster than the geometric decay of the numerator term $(\mu\phi)^{N+1}$ for sufficiently large N. This confirms the high-precision spectral convergence of the proposed method for analytic solutions. □

Lemma 2 (Fractional Markov–Bernstein Bound for Shifted Lucas Polynomials). *Let $\alpha \in (0,1)$. For the shifted Lucas polynomial $L_n^*(t)$ on $[0,1]$, the Caputo fractional derivative satisfies:*

$$\| D^\alpha L_n^* \|_\infty \leq \frac{4\, n^2\, \phi^n}{\Gamma(2-\alpha)}, \quad \forall\, n \geq 1, \tag{45}$$

where $\phi = \frac{1+\sqrt{5}}{2}$ is the golden ratio.

Proof. From the Caputo definition (1), for any $t \in [0,1]$:

$$|D^\alpha L_n^*(t)| \leq \frac{1}{\Gamma(1-\alpha)} \left\| \frac{d}{d\tau} L_n^* \right\|_\infty \int_0^t (t-\tau)^{-\alpha}\, d\tau. \tag{46}$$

Evaluating the integral yields $\int_0^t (t-\tau)^{-\alpha}\, d\tau = \frac{t^{1-\alpha}}{1-\alpha} \leq \frac{1}{1-\alpha}$. By Markov's inequality on $[0,1]$ [22], the integer-order derivative satisfies $\| (L_n^*)' \|_\infty \leq 2n^2 \| L_n^* \|_\infty$. Substituting the uniform bound from Lemma 1, $\| L_n^* \|_\infty \leq 2\phi^n$, we obtain:

$$\| D^\alpha L_n^* \|_\infty \leq \frac{4\, n^2\, \phi^n}{(1-\alpha)\,\Gamma(1-\alpha)} = \frac{4\, n^2\, \phi^n}{\Gamma(2-\alpha)}. \tag{47}$$

While the truncation error analysis provides a theoretical convergence rate for the solution coefficients, the Residual Error serves as a practical measure of how well the approximate solution satisfies the governing fractional differential equations. In the following, we derive an upper bound for the residual error norm.

Theorem 6 (Residual Error Bound). *Let $A_N(t)$ and $S_N(t)$ be the SLSCM approximate solutions. Under the assumptions of Theorem 5, and assuming the variable coefficients are bounded such that $\max_t |k(t)| \leq M_k$, the residual error $Res_N(t)$ satisfies the following asymptotic bound:*

$$\| Res_N \|_\infty \leq C \cdot \frac{(\mu\phi)^{N+1}}{(N-1)!}, \tag{48}$$

where C is a positive constant and ϕ is the golden ratio.

Proof. Define the residual function for the first governing equation, without loss of generality, as:

$$Res_A(t) = D^\alpha A_N(t) + \mu_A A_N(t) + k_S(t) S_N(t). \tag{49}$$

Subtracting the exact equation $0 = D^{\alpha}A(t) + \mu_A A(t) + k_S(t)S(t)$, we express the residual in terms of the truncation errors $e_A(t) = A(t) - A_N(t)$ and $e_S(t) = S(t) - S_N(t)$:

$$Res_A(t) = -D^{\alpha}e_A(t) - \mu_A e_A(t) - k_S(t)e_S(t). \tag{50}$$

Taking the uniform norm over $[0,1]$ and applying the triangle inequality:

$$\| Res_A \|_{\infty} \leq \| D^{\alpha}e_A \|_{\infty} + |\mu_A| \| e_A \|_{\infty} + M_{k_S} \| e_S \|_{\infty}. \tag{51}$$

We have already established the bound for $\| e_A \|_{\infty}$ in Theorem 5. Recalling the series representation:

$$D^{\alpha}e_A(t) = \sum_{n=N+1}^{\infty} a_n D^{\alpha}L_n^*(t). \tag{52}$$

Invoking the fractional Markov–Bernstein bound established in Lemma 2, we have

$$\| D^{\alpha}L_n^* \|_{\infty} \leq C_{\alpha} n^2 \phi^n. \tag{53}$$

where $C_{\alpha} = 4/\Gamma(2-\alpha)$. Substituting the coefficient bound $|a_n| \leq \frac{\mu^n}{n!}$:

$$\| D^{\alpha}e_A \|_{\infty} \leq \sum_{n=N+1}^{\infty} \frac{\mu^n}{n!}(C_{\alpha}n^2\phi^n) = C_{\alpha} \sum_{n=N+1}^{\infty} \frac{n^2(\mu\phi)^n}{n!}. \tag{54}$$

Since $\frac{n^2}{n!} = \frac{n}{(n-1)!}$ the series is dominated by its first term ($n = N+1$) for large N:

$$\| D^{\alpha}e_A \|_{\infty} \lesssim C_{\alpha} \frac{(N+1)^2(\mu\phi)^{N+1}}{(N+1)!} \leq C_{\alpha} \frac{(N+1)(\mu\phi)^{N+1}}{N!} \leq C_{\alpha} \frac{(\mu\phi)^{N+1}}{(N-1)!}. \tag{55}$$

Comparing this to the non-derivative term $\| e_A \|_{\infty} \sim \frac{(\mu\phi)^{N+1}}{(N+1)!}$, we observe that the derivative term dominates the error due to the smaller factorial in the denominator.

Finally, substituting back into Eq. (48), the total residual norm is bounded by the dominant term:

$$\| Res_A \|_{\infty} \leq C \frac{(\mu\phi)^{N+1}}{(N-1)!}. \tag{56}$$

Since the factorial function $(N-1)!$ grows significantly faster than the geometric term $(\mu\phi)^{N+1}$, the residual error converges to zero super-geometrically as $N \to \infty$. □

Remark 1 (Convergence for Non-Smooth Solutions). *Theorem 5 guarantees super-geometric convergence only under the assumption that the exact solution $A(t)$ is analytic (C^{∞}) on $[0,1]$. However, for fractional differential equations, the exact solution typically behaves as $u(t) \sim ct^{\alpha}$ near the origin, which implies limited regularity ($u(t) \in C^0[0,1]$ but $u'(t)$ is singular at $t = 0$). In such realistic scenarios, the convergence rate of polynomial spectral methods degrades from exponential to algebraic, due to the limited regularity of the solution at the origin. This aligns with the numerical saturation observed for $\alpha < 1$ in the subsequent results section.*

A natural measure of convergence is the difference between successive truncated expansions A $A_N(t)$ and $A_{N+1}(t)$. In the following, we derive an upper bound for this consecutive difference, demonstrating that the sequence of partial sums forms a Cauchy sequence in the Banach space $C[0,1]$.

Theorem 7 (Consecutive Approximation Error Bound). *Let $A_N(t)$ and $A_{N+1}(t)$ denote the truncated shifted Lucas expansions of the exact solution at degrees N and $N+1$, respectively. Assuming the exact solution is analytic with spectral coefficients satisfying the decay condition $|c_k| \leq \frac{\mu^k}{k!}$, the supremum norm of the consecutive difference satisfies the following asymptotic bound:*

$$\| A_{N+1} - A_N \|_\infty \leq \frac{2(\mu\phi)^{N+1}}{(N+1)!}, \tag{57}$$

where $\phi = \frac{1+\sqrt{5}}{2}$ *is the golden ratio. Consequently, the error decays super-geometrically as* $N \to \infty$.

Proof. Consider two successive truncations at N and $N+1$. Due to the linearity of the basis expansion, the difference function $E_{N,N+1}(t)$ is determined solely by the $(N+1)$-th spectral mode:

$$E_{N,N+1}(t) \coloneqq A_{N+1}(t) - A_N(t) = c_{N+1} L^*_{N+1}(t). \tag{58}$$

Taking the uniform norm over the domain $t \in [0,1]$, we have:

$$\| E_{N,N+1} \|_\infty = |c_{N+1}| \cdot \| L^*_{N+1} \|_\infty. \tag{59}$$

We now invoke the fundamental bounds established in Lemma 1 and Theorem 4. Substituting these estimates yields:

$$\| A_{N+1} - A_N \|_\infty \leq \left(\frac{\mu^{N+1}}{(N+1)!} \right) (2\phi^{N+1}) = 2\frac{(\mu\phi)^{N+1}}{(N+1)!}. \tag{60}$$

To elucidate the rate of convergence, we analyze the asymptotic behavior of the bound as $N \to \infty$. Utilizing Stirling's approximation for the factorial, $(N+1)! \sim \sqrt{2\pi(N+1)} \left(\frac{N+1}{e}\right)^{N+1}$, the bound behaves as:

$$\text{Bound}_N \approx \frac{2}{\sqrt{2\pi(N+1)}} \left(\frac{\mu\phi e}{N+1} \right)^{N+1}. \tag{61}$$

Since the base of the geometric term approaches zero ($\frac{\mu\phi e}{N+1} \to 0$) as N increases, the consecutive error decays faster than any exponential function.

This super-geometric decay implies that $\sum_{N=0}^{\infty} \| A_{N+1} - A_N \|_\infty < \infty$, proving that $\{A_N\}_{N \geq 0}$ is a Cauchy sequence in $C[0,1]$. This theoretically guarantees the uniform convergence of the SLSCM solution to the exact limit. □

6. Stability Analysis of the Equilibrium

A key characteristic of the classical Lanchester combat model is the instability of the trivial equilibrium $(A, S) = (0,0)$, which represents mutual annihilation. This saddle-point behavior leads to the deterministic victory of one force. In this section, we extend this stability analysis to the fractional-order model with variable coefficients. Due to the time-varying nature of $k_A(t)$ and $k_S(t)$, a complete analytical treatment of the non-autonomous system is challenging. Therefore, we analyze the *averaged autonomous system* to obtain essential insight into the local dynamics near the origin.

We consider the time-averages of the combat effectiveness coefficients over the operational timeframe $[0, T]$:

$$\bar{k}_A = \frac{1}{T} \int_0^T k_A(\tau)\, d\tau, \qquad \bar{k}_S = \frac{1}{T} \int_0^T k_S(\tau)\, d\tau. \tag{62}$$

The associated autonomous fractional system is:

$$\begin{aligned} D^\alpha A(t) &= -\bar{k}_S S(t) - \mu_A A(t), \\ D^\alpha S(t) &= -\bar{k}_A A(t) - \mu_S S(t). \end{aligned} \tag{63}$$

This system can be written in matrix form as $D^\alpha \boldsymbol{X}(t) = \boldsymbol{J}\boldsymbol{X}(t)$, where $\boldsymbol{X}(t) = [A(t), S(t)]^\top$ and

$$\boldsymbol{J} = \begin{bmatrix} -\mu_A & -\bar{k}_S \\ -\bar{k}_A & -\mu_S \end{bmatrix}. \tag{64}$$

The stability of the equilibrium $\boldsymbol{X} = \boldsymbol{0}$ for this linear fractional system is governed by the eigenvalues λ_1, λ_2 of the matrix $\boldsymbol{J}$. The characteristic equation is $\det(\boldsymbol{J} - \lambda \boldsymbol{I}) = 0$, which expands to:

$$\lambda^2 + (\mu_A + \mu_S)\lambda + (\mu_A \mu_S - \bar{k}_A \bar{k}_S) = 0. \tag{65}$$

The eigenvalues are given by:

$$\lambda_{1,2} = \frac{-(\mu_A + \mu_S) \pm \sqrt{(\mu_A + \mu_S)^2 - 4(\mu_A \mu_S - \bar{k}_A \bar{k}_S)}}{2}. \tag{66}$$

Under the physically realistic assumption that combat effectiveness dominates operational attrition, i.e., $\bar{k}_A \bar{k}_S > \mu_A \mu_S$, the discriminant satisfies:

$$\Delta = (\mu_A + \mu_S)^2 - 4(\mu_A \mu_S - \bar{k}_A \bar{k}_S) > (\mu_A + \mu_S)^2. \tag{67}$$

Consequently, $\sqrt{\Delta} > (\mu_A + \mu_S)$, guaranteeing one strictly positive and one strictly negative real eigenvalue:

$$\lambda_1 > 0, \quad \lambda_2 < 0. \tag{68}$$

The fundamental stability theorem for linear fractional differential systems of order $\alpha \in (0,1]$ is due to Matignon [16].

Theorem 8 (Matignon's Theorem). *Consider the linear fractional system $D^{\alpha}\boldsymbol{X}(t) = \boldsymbol{J}\boldsymbol{X}(t)$, where $\alpha \in (0,1]$. The equilibrium $\boldsymbol{X} = \boldsymbol{0}$ is asymptotically stable if and only if*

$$|\arg(\lambda_i)| > \frac{\alpha\pi}{2}, \quad \text{for all eigenvalues } \lambda_i \text{ of } \boldsymbol{J}. \tag{69}$$

If there exists an eigenvalue λ_i such that $|\arg(\lambda_i)| < \frac{\alpha\pi}{2}$, then the equilibrium is unstable.

Applying this theorem to our averaged system is straightforward. Since $\lambda_1 > 0$ and $\lambda_2 < 0$ are both real, their arguments are $\arg(\lambda_1) = 0$ and $\arg(\lambda_2) = \pi$. Therefore,

$$|\arg(\lambda_1)| = 0 < \frac{\alpha\pi}{2} \quad \text{for all } \alpha \in (0,1], \quad \text{while } |\arg(\lambda_2)| = \pi > \frac{\alpha\pi}{2}. \tag{70}$$

The presence of the eigenvalue λ_1 with $|\arg(\lambda_1)| < \alpha\pi/2$ immediately implies the following result.

Theorem 9 (Instability of the Origin). *For the averaged fractional Lanchester system of order $\alpha \in (0,1]$, if the averaged combat effectiveness satisfies $\bar{k}_A \bar{k}_S > \mu_A \mu_S$, then the equilibrium point $(A, S) = (0,0)$ is a saddle point and is unstable.*

Proof. The condition $\bar{k}_A \bar{k}_S > \mu_A \mu_S$ ensures that the matrix $\boldsymbol{J}$ has a real, positive eigenvalue λ_1. By Matignon's theorem, since $|\arg(\lambda_1)| = 0 < \alpha\pi/2$ for any $\alpha \in (0,1]$, the equilibrium is unstable. The fact that the other eigenvalue λ_2 is real and negative confirms the saddle-point structure. □

7. Numerical Results and Discussion

In this section, we present a comprehensive numerical assessment of the proposed Shifted Lucas Spectral Collocation Method (SLSCM) applied to the generalized fractional Lanchester combat model. All numerical experiments were conducted using the Google Colab cloud computing environment. The simulations were executed on a virtual workstation running Ubuntu 22.04.5 LTS, equipped with an Intel(R) Xeon(R) CPU 2.20GHz (2 vCPUs) and approximately 13 GB of RAM. The proposed SLSCM algorithms were implemented in Python 3.10, utilizing double-precision arithmetic for all matrix computations.

To evaluate the performance of the proposed scheme under realistic operational conditions, we consider a specific combat scenario characterized by time-dependent effectiveness coefficients. The Air Defense effectiveness $k_A(t)$ is modeled as a periodic function simulating environmental cycles or shift changes, while the Swarm effectiveness $k_S(t)$ follows an exponential decay simulating resource depletion or communication jamming. The functional forms are

defined as:

$$k_A(t) = k_A^0(1 + \delta_A \sin(\omega_A t)), \qquad k_S(t) = k_S^0 e^{-\lambda_S t}. \tag{71}$$

Unless otherwise stated, the model parameters and initial conditions used throughout the simulations are listed in Table 1.

Table 1: Parameter values and initial conditions employed for the numerical simulations.

Parameter	Physical Interpretation	Value
A_0	Initial Air Defense strength	100.0
S_0	Initial Swarm/Drone strength	80.0
μ_A	Operational attrition rate (Air Defense)	0.02
μ_S	Operational attrition rate (Swarm)	0.03
k_A^0	Base effectiveness (Air Defense)	0.05
k_S^0	Base effectiveness (Swarm)	0.04
δ_A	Amplitude of periodic variation	0.2
ω_A	Frequency of variation	4π
λ_S	Decay rate of Swarm effectiveness	0.5

Our analysis focuses on four key aspects:

i. validation against high-order reference solutions for the integer-order case.

ii. the impact of memory effects on combat dynamics.

iii. verification of theoretical stability conditions.

iv. computational efficiency benchmarking against standard solvers.

To validate the accuracy of the proposed scheme, we first consider the classical integer-order limit ($\alpha = 1$), where the system reduces to a system of Ordinary Differential Equations (ODEs). In the absence of an exact analytical solution for the variable-coefficient case, we utilize a reference solution obtained via the *DOP853* integrator (an explicit Runge-Kutta method of order 8) with stringent tolerance settings ($Atol = Rtol = 10^{-14}$).

Table 2 presents the maximum pointwise error norms $\| A_N - A_{ref} \|_\infty$ and $\| S_N - S_{ref} \|_\infty$ for different N. The characteristic of spectral convergence is evident in the results: the error decreases exponentially until it reaches a saturation plateau (about 10^{-12}) dictated by the accuracy of the reference solution (Atol = Rtol = 10^{-14}). The method demonstrates the efficiency of the Lucas basis for smooth dynamical systems by achieving engineering accuracy (10^{-6}) with as few as $N = 10$ collocation nodes.

Table 2: Maximum L_∞ error norms for the SLSCM approximation ($\alpha = 1$) compared to the reference DOP853 solution.

Degree	Air Defense $A(t)$		Swarm Units $S(t)$	
N	$\| E_A \|_\infty$	CPU Time (s)	$\| E_S \|_\infty$	CPU Time (s)
4	2.90×10^{-3}	0.0002	3.35×10^{-1}	0.0002
8	5.53×10^{-5}	0.0003	8.33×10^{-3}	0.0003
12	5.24×10^{-7}	0.0003	4.47×10^{-5}	0.0003
16	9.99×10^{-10}	0.0005	8.31×10^{-8}	0.0005

Degree N	Air Defense $A(t)$		Swarm Units $S(t)$	
	$\| E_A \|_\infty$	CPU Time (s)	$\| E_S \|_\infty$	CPU Time (s)
20	3.87×10^{-12}	0.0006	6.84×10^{-10}	0.0006

The exponential decay behaviour is visually confirmed in Fig. 1, where the error curves appear linear on a semi-logarithmic scale before saturation due to round-off errors.

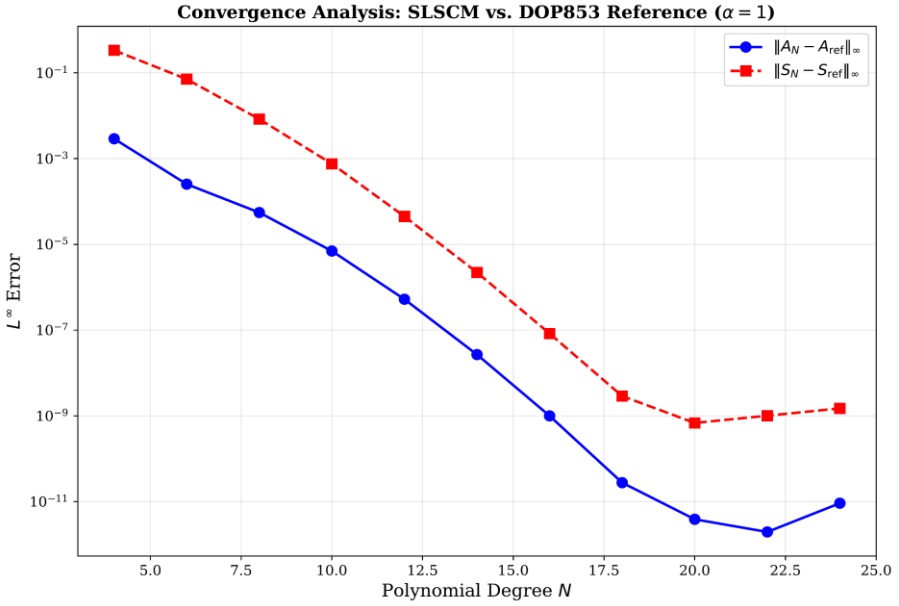

Figure 1: Spectral convergence of the SLSCM solution for $\alpha = 1$. The semi-logarithmic plot demonstrates the exponential decay of the error $\| \boldsymbol{u}_N - \boldsymbol{u}_{ref} \|_\infty$ with respect to the polynomial degree N.

We investigate the impact of the fractional order $\alpha \in \{0.5, 0.7, 0.9, 1.0\}$ on the combat attrition dynamics. Figure 2 illustrates the temporal evolution of Air Defense forces $A(t)$ and Swarm units $S(t)$.

Two distinct physical phenomena characteristic of fractional calculus are observed:

I. Memory Shock (Short-time behavior): As α decreases, the initial rate of attrition increases significantly (steeper slope at $t \to 0^+$). This reflects the "heavy" weight assigned to the initial state by the singular kernel $t^{-\alpha}$, simulating an intense initial engagement or shock.

II. Heavy Tail (Long-time behavior): Conversely, at later times, the decay rate for fractional orders becomes slower than the integer case. Physically, this implies that systems with memory ($\alpha < 1$) exhibit a form of inertia or hereditary resistance; past survival contributes to current persistence, leading to a "heavy tail" in the force strength trajectory.

To verify the instability of the mutual annihilation equilibrium predicted in Section 6, we computed the eigenvalues of the averaged Jacobian matrix $\boldsymbol{J}$, with the time-averages evaluated over the collocation domain $T = 1$. For the resulting parameters $\bar{k}_A = 0.05$ and $\bar{k}_S \approx 0.031$, the eigenvalues were found to be:

$$\lambda_1 \approx +0.0150, \quad \lambda_2 \approx -0.0650. \tag{72}$$

The existence of a strictly positive eigenvalue λ_1 confirms that the origin is a saddle point and is unstable in the Lyapunov sense [22]. According to Matignon's theorem, since $|\arg(\lambda_1)| = 0 < \alpha\pi/2$, the system remains unstable for all tested α.

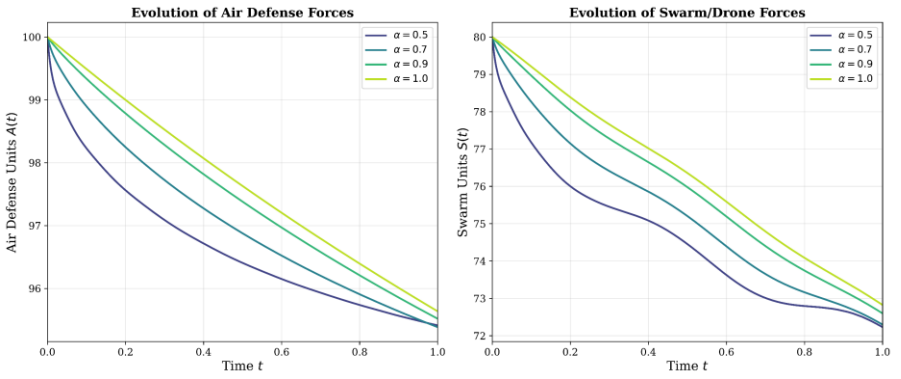

Figure 2: Time evolution of combat forces for varying fractional orders α. Lower α values induce a faster initial decline followed by a slower asymptotic decay, illustrating the non-local memory effects.

Figure 3 visualizes the phase plane trajectories. Regardless of the fractional order, the state vector $[A(t), S(t)]^T$ is repelled from the origin $(0,0)$, confirming that a stalemate, total mutual destruction, is structurally unstable and that the system will inevitably evolve towards the victory of one side.

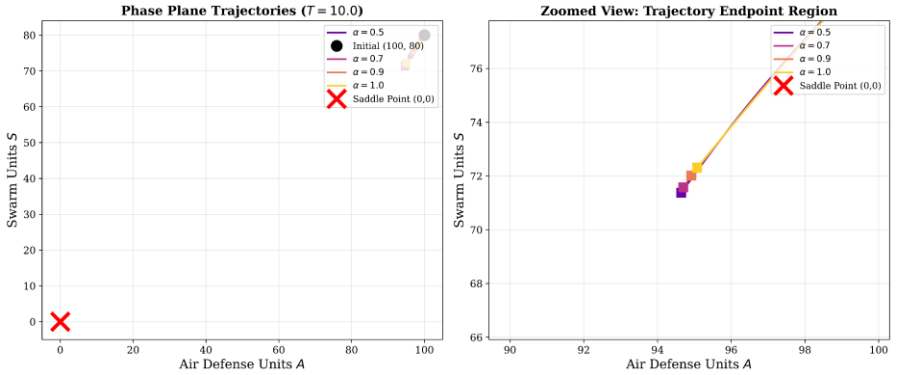

Figure 3: Phase plane trajectories for $t \in [0,10]$.

To rigorously quantify the computational advantages of the proposed framework, we conducted a comparative efficiency analysis against three industry-standard adaptive integrators from the *SciPy* library: *RK45* (explicit Runge-Kutta-Fehlberg order 5(4)), *DOP853* (explicit Runge-Kutta order 8), and *BDF* (Backward Differentiation Formula for stiff systems). The results are visualized in Figure 4, which dissects the performance into two complementary metrics: the cost-accuracy trade-off and a combined efficiency index.

Figure 4(a) illustrates the L_∞ error norm as a function of CPU execution time (in seconds) on a double-logarithmic scale. The SLSCM (represented by the blue curve) exhibits a distinct "Pareto-optimal" behavior, occupying the bottom-left region of the plot. While low-order methods like *RK45* and *BDF* are competitive for coarse tolerances (10^{-2}–10^{-3}), their computational cost scales unfavorably when higher precision is demanded. In sharp contrast, the SLSCM demonstrates a steep spectral descent, achieving high-precision results ($< 10^{-10}$) in the millisecond regime ($t_{cpu} \approx 10^{-2}$ s). Notably, to achieve an error of 10^{-9}, the standard *DOP853* integrator requires nearly an order of magnitude more computational time compared to the spectral approach.

To further formalize this comparison, Figure 4(b) presents the *Efficiency Index* ($\mathcal{E}$), defined as the product of the global error and the CPU time ($\mathcal{E} = \| \boldsymbol{E} \|_\infty \times t_{cpu}$). Lower values of $\mathcal{E}$ indicate a more efficient algorithm that balances accuracy with speed. The plot reveals that the SLSCM minimizes this index significantly, reaching values as low as 10^{-12} for $N \geq 16$. This implies that the marginal cost of increasing accuracy in the spectral framework is negligible compared to the iterative refinement required by time-stepping schemes. This efficiency stems directly from the global nature of the method: solving the fractional system is reduced to a single algebraic matrix inversion via the Exact Operational Matrix, avoiding the cumulative overhead of thousands of sequential time steps required to resolve the non-local memory integral in classical solvers.

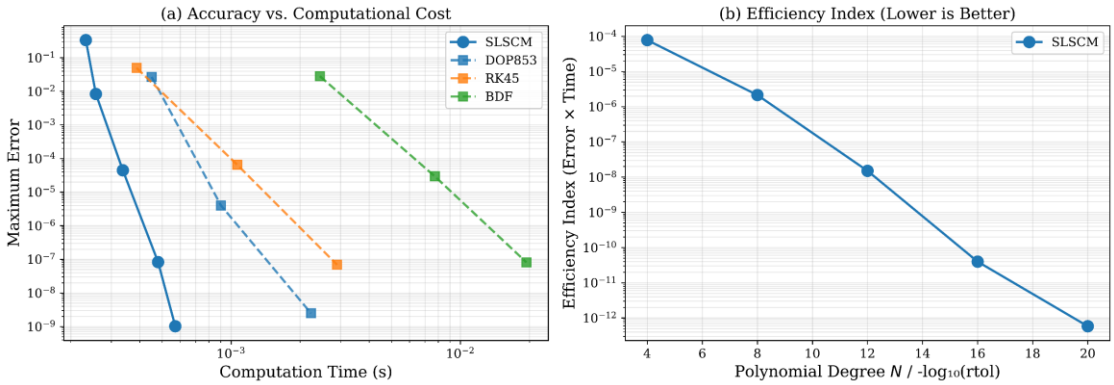

Figure 4: Computational efficiency analysis: ***(a)*** *Accuracy vs. Computational Cost.* ***(b)*** *Efficiency Index (Error × Time).*

Finally, we assess the global consistency of the solution for the fractional case ($\alpha < 1$) where no exact reference exists. We compute the residual error $R(t)$ on a dense grid of points distinct from the collocation nodes.

Figure 5 depicts the pointwise residual errors $|R_A(t)|$ and $|R_S(t)|$ across the time domain for varying polynomial degrees. For the smooth case ($\alpha = 1.0$), the residuals drop rapidly below 10^{-12} as N increases to 20, indicating a near-exact reconstruction of the ODE dynamics.

For the fractional case ($\alpha = 0.7$), the residuals are significantly higher ($\approx 10^{-3}$) and exhibit peaks near the boundaries. This behavior is a direct consequence of the singularity at $t = 0$, which introduces a limited regularity that decays slowly despite increasing N.

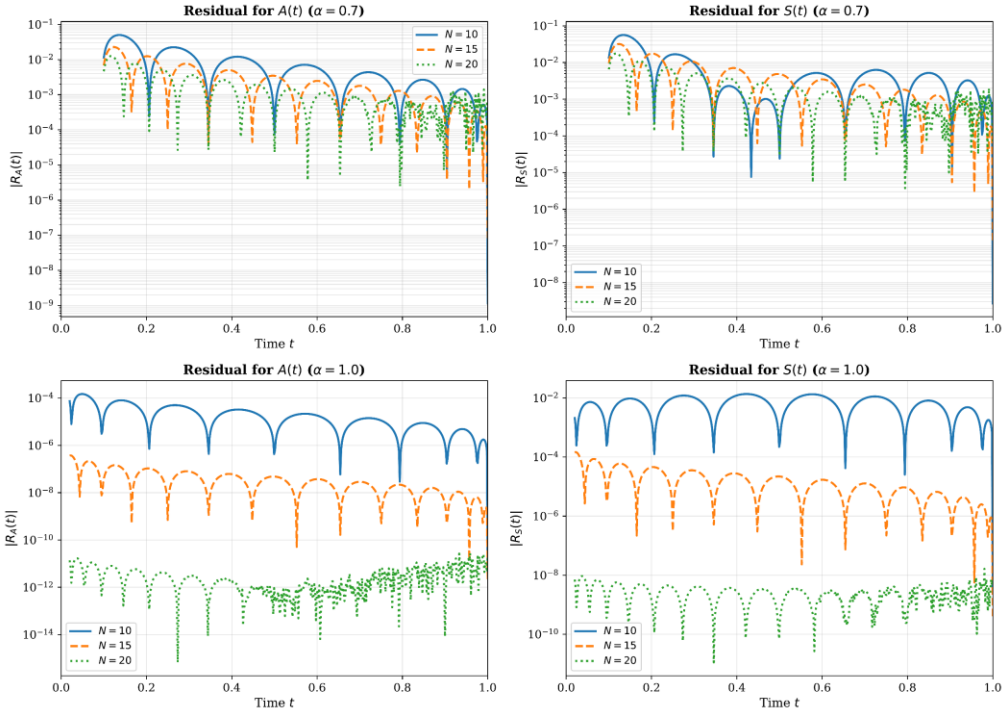

Figure 5: Pointwise residual error profiles for $A(t)$ and $S(t)$ over the time domain $[0,1]$.

Furthermore, Figure 6 summarizes the convergence of the maximum residual norm $\| R \|_\infty$ with respect to N. It reveals a critical distinction between the integer and fractional cases:

- For $\alpha = 1.0$, the residual decays exponentially to a saturation level of approximately 10^{-8}, at which point round-off amplification through the operational matrix limits further improvement.

- For $\alpha < 1.0$, the residual convergence saturates at an algebraic rate (approx. 10^{-2}–10^{-3}).

This saturation is expected and is not a failure of the method, but rather a consequence of the weak singularity of the fractional solution at $t = 0$ (where $y(t) \sim t^{\alpha}$). Since the standard polynomial basis consists of smooth functions, it struggles to resolve the t^{α} singularity with spectral accuracy.

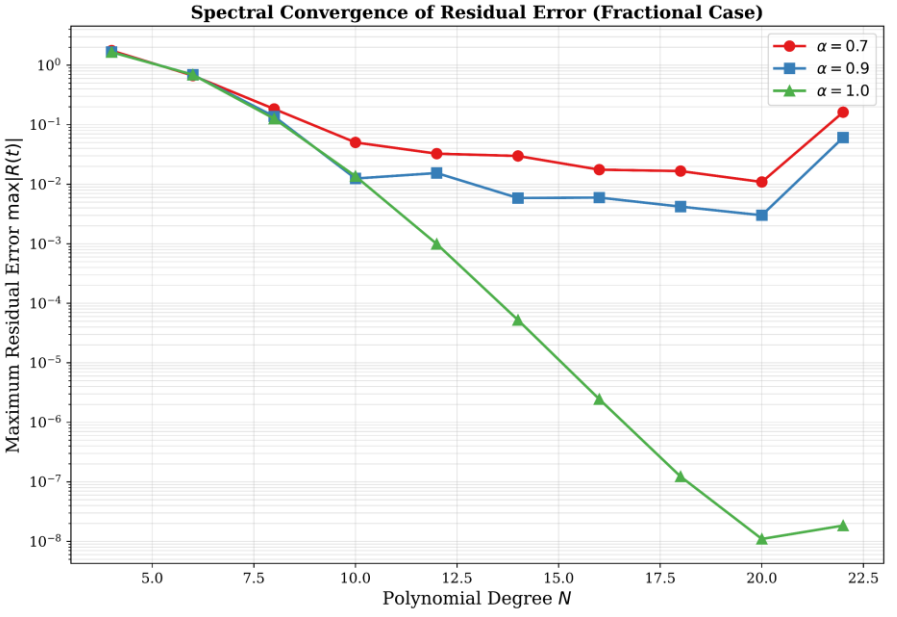

Figure 6: Maximum residual error vs. polynomial degree N.

8. Conclusion

This work developed a Shifted Lucas Spectral Collocation Method (SLSCM) for the generalized fractional-order Lanchester combat model with time-dependent variable coefficients. The principal contributions are:

(i) A closed-form operational matrix for the Caputo derivative of shifted Lucas polynomials via Gauss hypergeometric functions;

(ii) Well-posedness with explicit Mittag-Leffler bounds (Theorem 3);

(iii) Rigorous confirmation of the saddle-point instability via Matignon's theorem (Theorem 9); and (iv) error estimates establishing super-geometric convergence for analytic solutions (Theorems 5–7). Numerical experiments demonstrated spectral convergence to $\mathcal{O}(10^{-12})$ with $N = 20$ for $\alpha = 1$, while for $\alpha < 1$ the method captured memory-induced initial shock and heavy-tail decay, outperforming RK45, DOP853, and BDF by orders of magnitude in the high-precision regime.

Convergence saturates to an algebraic rate for fractional orders due to the weak singularity $u(t) \sim t^{\alpha}$ at the origin. Future directions include fractional polynomial bases or graded meshes to recover spectral convergence for $\alpha < 1$, extension to nonlinear multi-force systems, stochastic perturbations, and inverse parameter identification.

References

[1] F. W. Lanchester, 1916, *Aircraft in Warfare: The Dawn of the Fourth Arm*, Constable and Company Limited, London

[2] A. Washburn, M. Kress, 2009, *Combat Modeling*, Springer, New York

[3] I. Podlubny, 1999, *Fractional Differential Equations*, Academic Press, San Diego

[4] X. Wang, Y. Zhang, S. Shen, Fractional-order Lanchester combat model with delay, *Def. Technol.,* Vol. 17, No. 4, pp. 1415-1423, 2021.

[5] M. Kress, I. Talmor, A new look at the 3:1 rule of combat, *J. Oper. Res. Soc.,* Vol. 60, No. 8, pp. 1076-1082, 2009.

[6] K. Diethelm, 2010, *The Analysis of Fractional Differential Equations*, Springer, Berlin

[7] L. N. Trefethen, 2000, *Spectral Methods in MATLAB*, SIAM, Philadelphia
[8] J. Shen, T. Tang, L. Wang, 2011, *Spectral Methods: Algorithms, Analysis and Applications*, Springer Science & Business Media,
[9] W. M. Abd-Elhameed, Y. H. Youssri, New connection formulae between Chebyshev and Lucas polynomials: New expressions involving Lucas numbers via hypergeometric functions, *Adv. Stud. Contemp. Math.,* Vol. 28, No. 3, pp. 357-368, 2018.
[10] M. H. Salama, H. A. Zedan, W. M. Abd-Elhameed, Y. H. Youssri, Galerkin method with modified shifted lucas polynomials for solving the 2d poisson equation, *J. Comput. Appl. Mech,* Vol. 56, pp. 737-775, 2025.
[11] M. H. Salama, H. A. Zedan, W. M. Abd-Elhameed, Y. H. Youssri, Spectral Treatment of the Fractional Bratu Equation via Shifted Lucas Polynomials: A Precise Collocation Approach with Error Quantification, *Contemp. Math.,* Vol. 6, No. 5, pp. 6832-6870, 2025.
[12] W. M. Abd-Elhameed, Y. H. Youssri, A. G. Atta, Tau algorithm for fractional delay differential equations utilizing seventh-kind Chebyshev polynomials, *J. Math. Model.,* Vol. 12, No. 2, pp. 277-299, 2024.
[13] Y. H. Youssri, W. M. Abd-Elhameed, H. M. Ahmed, New fractional derivative expression of the shifted third-kind Chebyshev polynomials: Application to a type of nonlinear fractional pantograph differential equations, *J. Funct. Spaces,* Vol. 2022, pp. 9836512, 2022.
[14] W. M. Abd-Elhameed, Y. H. Youssri, New formulas of the high-order derivatives of fifth-kind Chebyshev polynomials: Spectral solution of the convection-diffusion equation, *Numer. Methods Partial Differ. Equ.,* Vol. 40, No. 2, 2024.
[15] Y. H. Youssri, A. G. Atta, Spectral Collocation Approach via Normalized Shifted Jacobi Polynomials for the Nonlinear Lane--Emden Equation with Fractal-Fractional Derivative, *Fractal and Fractional,* Vol. 7, No. 2, pp. 133, 2023.
[16] D. Matignon, Stability results for fractional differential equations with applications to control processing, in *Computational Engineering in Systems Applications*, Lille, France, 1996, pp. 963-968.
[17] H. J. Haubold, A. M. Mathai, R. K. Saxena, Mittag-Leffler functions and their applications, *J. Appl. Math.,* Vol. 2011, pp. 298628, 2011.
[18] H. Ye, J. Gao, Y. Ding, A generalized Gronwall inequality and its application to a fractional differential equation, *J. Math. Anal. Appl.,* Vol. 328, No. 2, pp. 1075-1081, 2007.
[19] W. M. Abd-Elhameed, Y. H. Youssri, Generalized Lucas polynomial sequence approach for fractional differential equations, *Nonlinear Dyn.,* Vol. 89, No. 2, pp. 1341-1355, 2017.
[20] W. M. Abd-Elhameed, O. M. Alqubori, A. G. Atta, A Collocation Procedure for Treating the Time-Fractional FitzHugh-Nagumo Differential Equation Using Shifted Lucas Polynomials, *Mathematics,* Vol. 12, No. 23, pp. 3672, 2024.
[21] J. P. Boyd, 2013, *Chebyshev and Fourier Spectral Methods: Second Revised Edition*, Dover Publications,
[22] Y. Li, Y. Chen, I. Podlubny, Mittag–Leffler stability of fractional order nonlinear dynamic systems, *Automatica,* Vol. 45, No. 8, pp. 1965-1969, 2009/08/01/, 2009.